

## Experimental Evaluation of $8 \times 4$ Eigenmode SDM Transmission in Broadband MIMO-OFDM Systems

*Kentaro Nishimori<sup>†</sup>, Riichi Kudo, Yasushi Takatori, and Koichi Tsunekawa*

### Abstract

We describe the features and basic characteristics of an  $8 \times 4$  MIMO-OFDM (multiple-input multiple-output orthogonal frequency division multiplexing) testbed that can evaluate eigenmode space division multiplexing (E-SDM) in broadband MIMO-OFDM systems. The testbed achieved a maximum frequency utilization of 13.7 bits/s/Hz, the highest value for transmission reported in a formal publication.

### 1. Introduction

Due to the recent popularity of mobile phones and broadband wireless local area networks (LANs), broadband wireless systems using orthogonal frequency division multiplexing (OFDM) were introduced to combat the effects of multi-path fading in indoor wireless LAN systems. Moreover, the multiple-input multiple-output (MIMO) technique is incorporated into these broadband wireless systems using OFDM to achieve higher transmission speeds without expanding the frequency band [1], [2].

MIMO technologies are categorized into 1) high-quality transmission of a single data stream as space time codes using transmit and receive diversity or 2) high-data-rate transmission of multiple data sub-streams [3], [4]. The latter, which is called space division multiplexing (SDM), is attractive because it improves the transmission rate in a limited frequency bandwidth. Moreover, various algorithms such as Zero Forcing (ZF), Minimum Mean Square Error (MMSE), Ordered Successive Cancellation (OSUC), and Maximum Likelihood Detection (MLD) have been proposed to discriminate the inter-substream interference if the transmitters cannot know the channel state information (CSI) [3].

On the other hand, if the transmitter can know the CSI, then Eigenmode-SDM (E-SDM) [5]-[7] is very effective because optimal MIMO transmission can be

achieved with simple spatial filtering using the ZF algorithm at the receiver, for example [7]. The channel capacity in MIMO channels can be improved without increasing the number of receive antennas if the number of transmit antennas is increased by using E-SDM. Thus, E-SDM is suitable for downlink systems, which need to provide high-data-rate transmission because the number of antennas is generally greater at the access point than at the mobile terminal.

To incorporate MIMO technologies into commercial wireless systems, several chip vendors, manufacturers, and research institutes around the world have developed prototypes with MIMO transmission ranging from  $2 \times 2$  to  $4 \times 4$  [8]-[11]. However, only a few studies have evaluated the frequency utilization for MIMO transmission in an actual environment. For example, a maximum frequency utilization of 2.7 bits/s/Hz can be obtained in commercial wireless LAN systems based on the IEEE.802.11a standard [12]. In the case of MIMO systems, it was reported that maximum frequency utilization of 10 bits/s/Hz was obtained with  $4 \times 4$  MIMO transmission using simple MLD without transmit beamforming [10].

To further improve the frequency utilization, it is effective to increase the number of antennas. However, it is very difficult to use more than four antennas at the mobile terminal because many terminal stations are small, such as PCMCIA (Personal Computer Memory Card International Association) cards or personal digital assistants (PDAs). Since E-SDM can achieve a high transmission rate without increasing the number of antennas at the mobile terminal, it is very effective to use E-SDM when the number of

<sup>†</sup> NTT Network Innovation Laboratories  
Yokosuka-shi, 239-0847 Japan  
E-mail: nishimori.kentaro@lab.ntt.co.jp

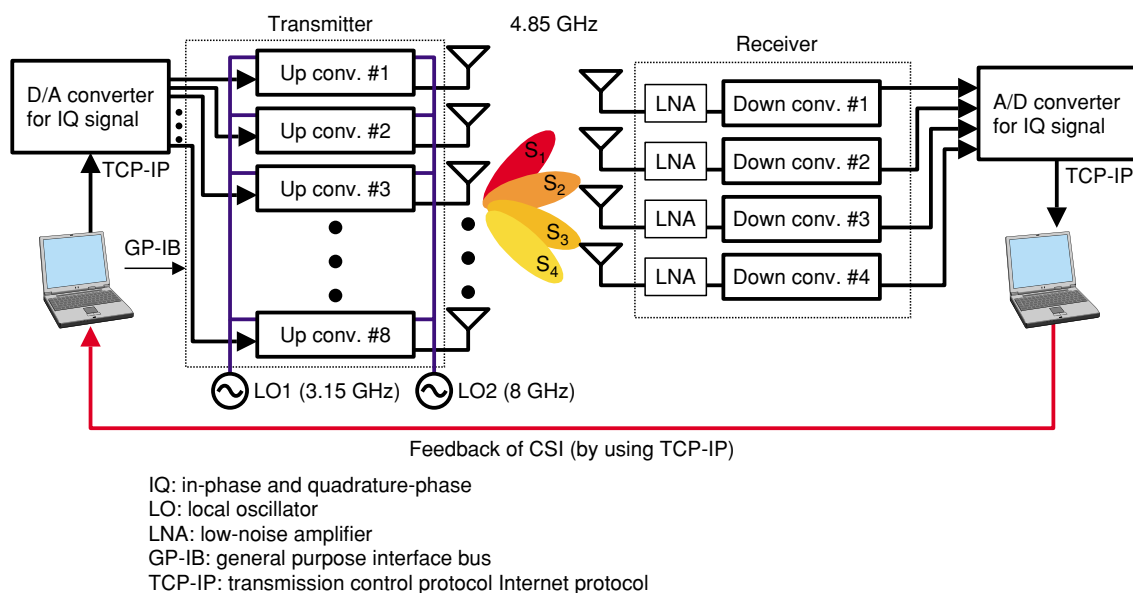


Fig. 1. Configuration of MIMO-OFDM transceiver.

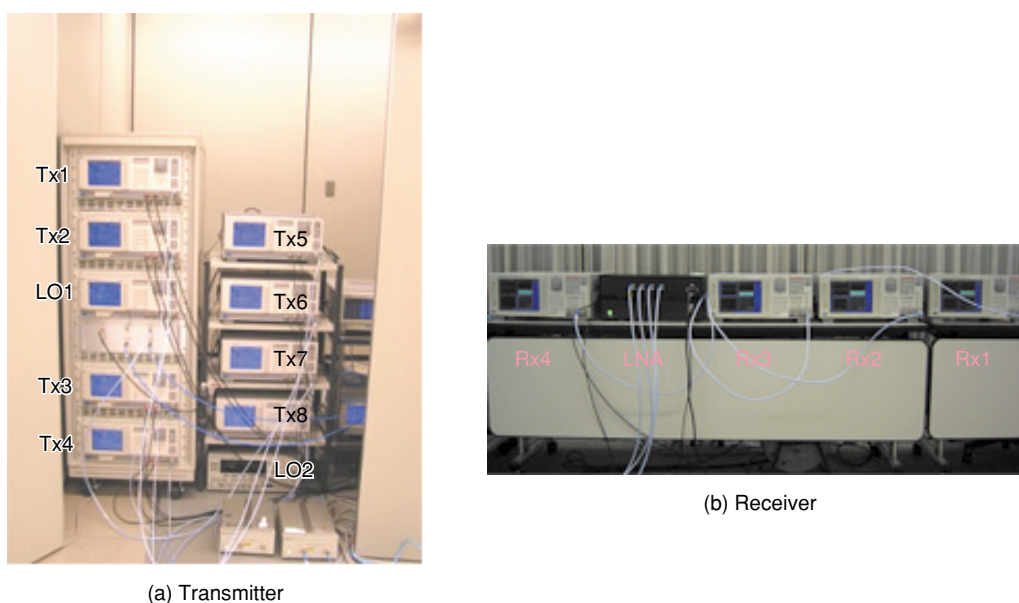


Fig. 2. Photograph MIMO-OFDM transceiver.

antennas at the access point is greater than four and the number of mobile terminals is less than four, especially from the viewpoint of the hardware implementation in near-future commercial systems.

In this paper, we describe the features and basic characteristics of a broadband MIMO-OFDM testbed that can evaluate transmit beamforming such as E-SDM. We set the numbers of transmit and receive antennas to eight and four, respectively, to clarify the effectiveness of our testbed using E-SDM for the pro-

totypes developed by outside research institutes. This testbed can also handle 100-MHz bandwidth signals. It can obtain not only spatial/frequency correlation and eigenvalue distributions, which are key parameters in MIMO channels, but also evaluate the transmission quality including error correction for MIMO-OFDM transmission. Finally, we report that a maximum frequency utilization of 13.7 bits/s/Hz, the highest value for a transmission yet reported in a formal publication related to MIMO technology, was

achieved with  $8 \times 4$  E-SDM transmission on the MIMO-OFDM testbed. Section 2 outlines the  $8 \times 4$  MIMO-OFDM testbed and communication flow. Section 3 presents experimental results for the bit error rate (BER) and frequency utilization when SDM and E-SDM with ZF were used for MIMO transmission.

## 2. Configuration of $8 \times 4$ MIMO-OFDM testbed

### 2.1 Hardware configuration

The configuration of the experimental testbed for broadband MIMO-OFDM transmission is shown in Fig. 1 and a photograph of it is shown in Fig. 2. Its main parameters are given in Table 1. The center frequency of this testbed is 4.85 GHz. To maximize the effectiveness of E-SDM transmission, we set the number of transmitters and receivers to eight and four, respectively. The maximum  $8 \times 4$  MIMO-OFDM transmission can be evaluated using a bandwidth of 100 MHz.

In the transmitters, the transmit signals are generated in a personal computer (PC), and uploaded to a digital/analog (D/A) converter as shown in Fig. 1. After D/A conversion of these signals, frequency

conversion is applied and the RF (radio frequency) signals at 4.85 GHz are transmitted. In the receivers, these signals are down-converted, and A/D conversion is applied. These signals are finally transferred to a PC. All the signal processing is performed off-line to evaluate the various SDM algorithms in our testbed. Moreover, as shown in Fig. 1, the CSI is transferred over a wired connection to determine the transmit weight in our MIMO-OFDM testbed.

As shown in Fig. 1, signal generators (LO1 and LO2) are used for the local oscillators to enhance the stability of the frequency converter among the transmitters or receivers. Each D/A converter has 128 Mbytes of memory, and signals with various formats can be evaluated. Each A/D converter has 128 Mbytes of memory, and we can handle data acquisition for six seconds at a maximum of 20 MHz, for example.

### 2.2 Communication flow of MIMO-OFDM testbed

In this sub-section, we describe the frame format, the scheme for estimating the channel matrix, and the communication flow used in our MIMO-OFDM testbed.

The frame format used to achieve  $8 \times 4$  transmit beamforming such as E-SDM in the MIMO-OFDM testbed is shown in Fig. 3. Its signal parameters are based on the IEEE802.11a standard, which is used for commercial wireless LANs. This frame format is extended to estimate the channel matrix for MIMO-OFDM transmission. When we use the SDM scheme without beamforming, the maximum number of transmit antennas is four because the number of receivers is four. Details of the frame format for  $4 \times 4$

Table 1. Parameters for MIMO-OFDM transceiver.

Number of antennas	8 (Tx), 4 (Rx)
Frequency	4.85 GHz
Bandwidth	100 MHz
Range of AD/DA	14 bits
Transmission power	0 dBm (without HPA)
Sensitivity	-20 to -70 dBm

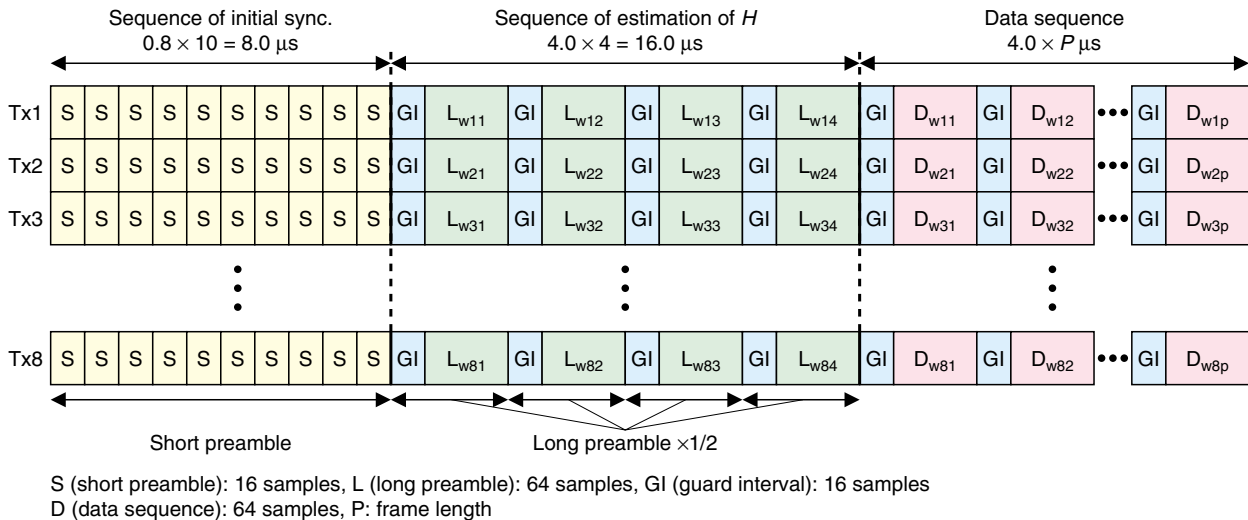


Fig. 3. Frame format for  $8 \times 4$  transmit beamforming.

MIMO-OFDM transmission are given in Refs. [13] and [14].

In Fig. 3, a short preamble is used for timing detection of the fast Fourier transform (FFT) window of the OFDM signals. Timing detection uses sliding correlation methods. Next, the channel matrix for the MIMO channels is estimated using a long preamble as shown in Fig. 3. Term  $L_{wmk}$  represents the OFDM signals, which are weighted with the  $m$ -th ( $m = 1 - 8$ ) transmit antenna obtained by multiplying the  $k$ -th ( $k = 1 - 4$ ) eigenvector and the long preamble.

In the data sequence,  $P$  OFDM symbols are transmitted per stream. The four pilot subcarriers are inserted in all OFDM symbols to compensate for the phase rotation, and the number of these pilot subcarriers

is given in **Table 2**. Term  $D_{wml}$  denotes the OFDM signals at the  $l$ -th ( $l = 1 - P$ ) timing, which is weighted by the  $m$ -th ( $m = 1 - 8$ ) transmit antenna obtained by multiplying the first and fourth eigenvectors and the first and fourth streams, respectively. We used the modulation schemes and coding rates given in Table 2.

The signal processing in our MIMO-OFDM testbed before D/A conversion and after A/D conversion is shown in **Figs. 4** and **5**, respectively. At the transmitter site in Fig. 4, the transmit bits are first divided into four streams, and convolutional coding with a constraint length of seven is used. Next, these bits are interleaved and modulated, and the signals are multiplied by the weights for transmit beamforming. In this paper, E-SDM is used for the transmit beamforming. The eigenvectors are obtained by singular decomposition of the channel matrix in E-SDM. The channel matrix  $H_k$  for subcarrier  $f_k$  is obtained through feedback from the receiver to the transmitter via the cable in the MIMO-OFDM testbed. The singular value decomposition is shown in the following equations.

Table 2. Parameters of MIMO-OFDM transmission.

Bandwidth	20 MHz
Sampling rate (A/D)	40 MHz
Sampling rate (D/A)	80 MHz
Number of FFT points	64
Number of subcarriers	48
Number of pilot subcarriers	4
Guard interval length	0.8 $\mu$ s
Effective signal length	3.2 $\mu$ s
Length of short preamble	2 OFDM symbols
Length of preamble	4 OFDM symbols
Modulation scheme	QPSK, 16QAM, 64QAM, 256QAM
Coding rate	1/2, 2/3, 3/4, 5/6, 7/8

$$H_k = U_k \sum_k V_k^H \tag{1}$$

$$U_k = [\mathbf{u}_{k,1} \mathbf{u}_{k,2}, \dots, \mathbf{u}_{k,L}] \tag{2}$$

$$V_k = [\mathbf{v}_{k,1} \mathbf{v}_{k,2}, \dots, \mathbf{v}_{k,L}] \tag{3}$$

$$\sum_k = \text{diag}[\sqrt{\lambda_{k,1}}, \sqrt{\lambda_{k,2}}, \dots, \sqrt{\lambda_{k,L}}], \tag{4}$$

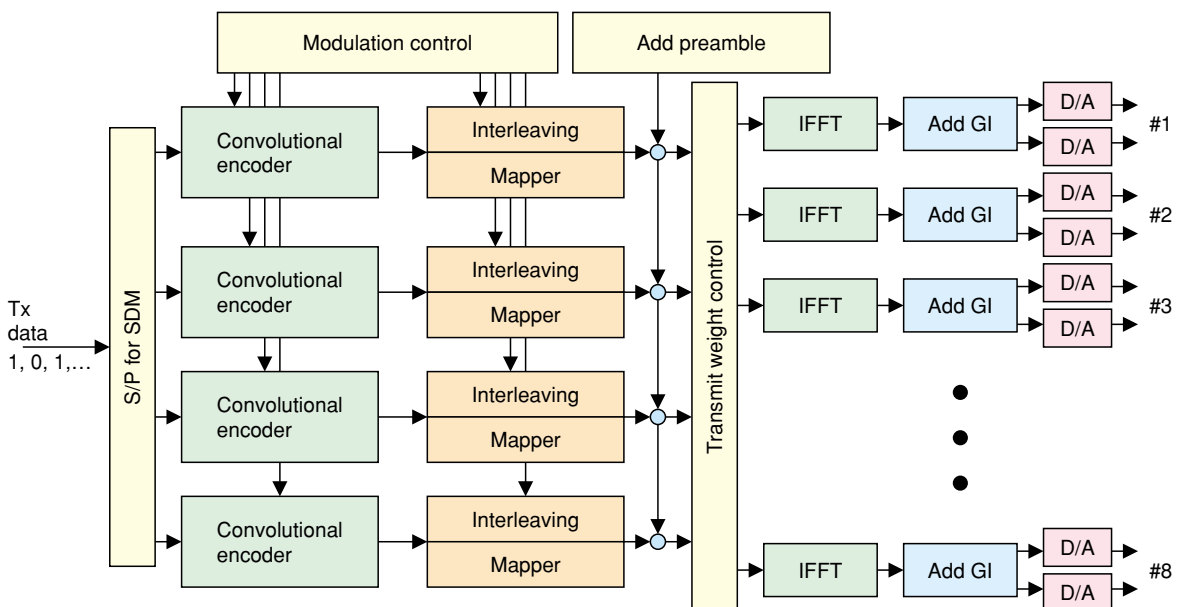


Fig. 4. Signal processing part before D/A converter.

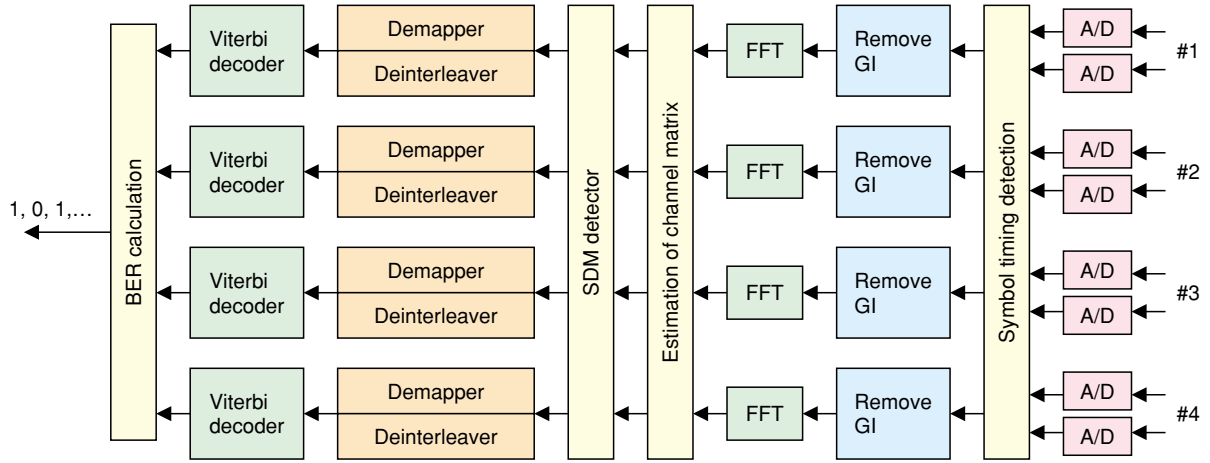


Fig. 5. Signal processing part after A/D converter.

where  $U_k$  and  $V_k$  denote the eigenvectors of the transmitter and receiver for subcarrier  $f_k$ , respectively. Eigenvector  $V_k$  is used as the transmit weight for subcarrier  $f_k$ . In addition,  $\Sigma_k$  represents the matrix whose diagonal terms consist of eigenvalues for subcarrier  $f_k$ , and the numbers of eigenvector beams, modulation schemes, and coding rates are generally determined according to the values of these eigenvalues for each subcarrier. In this paper, for simplicity, the number of eigenvector beams is fixed to four and three for  $8 \times 4$  and  $4 \times 4$  E-SDM, respectively. The modulation scheme and coding rate for each stream are also fixed among the subcarriers. Finally, the inverse fast Fourier transform (IFFT) process is applied to the signals after beamforming, and D/A conversion is performed.

At the receiver site in Fig. 5, the baseband signals are first converted to digital signals by the A/D converter after frequency conversion. Next, timing detection using the short preamble in Fig. 3 and FFT are applied to these signals after the guard interval has been removed. After FFT processing, the channel matrix is estimated by utilizing the sequence of the long preamble in Fig. 3, and the SDM decoding algorithm is applied using channel matrix  $H_k$  for subcarrier  $f_k$ . In this paper, the ZF algorithm is used as the SDM decoding algorithm. The decoding signals are given by the following equations:

$$\mathbf{Y}_k = (\mathbf{H}_k^H \mathbf{H}_k)^{-1} \mathbf{H}_k^H \mathbf{X}_k \quad (5)$$

$$\mathbf{X}_k = [x_{k,1}, \dots, x_{k,4}]^T \quad (6)$$

$$\mathbf{Y}_k = [y_{k,1}, \dots, y_{k,4}]^T, \quad (7)$$

where  $\mathbf{Y}_k$  and  $\mathbf{X}_k$  represent the decoded and received

signal vectors for subcarrier  $f_k$ , respectively. Finally, the de-interleaver and Viterbi decoder are used for these decoded signals, and the BER is calculated.

### 3. Experiment using MIMO-OFDM testbed

#### 3.1 Measurement environment

To clarify the basic characteristics of our MIMO-OFDM testbed, we conducted measurements in an indoor environment (Fig. 6). Sleeve antennas\* were used for the transmit and receive antennas. Rectangular and linear arrays were used for the transmit and receive arrays, respectively, which both had an element spacing of 1.0 wavelength. The heights of the transmit and receive antennas were 2.0 and 1.2 m, respectively. The total transmission power was 6 dBm, and the transmission power per antenna changed according to the number of antennas used. For example, when we used four transmit antennas, Antennas #1 to #4 in Fig. 6 were used. The transmit antennas were located at Point T and the receive antennas were located at the four points A to D. To clarify how the transmission quality depended on the direction of the receive array antenna, we evaluated four rotation angles ( $-45^\circ$ ,  $0^\circ$ ,  $45^\circ$ ,  $90^\circ$ ) at each receiving point.

Table 3 gives the combinations of the transmit and receive antennas and the SDM scheme at the transmitter and receiver. The BER and frequency utiliza-

\* Sleeve antennas: Sleeve antenna is generally used for the measurement antenna because this antenna has omni-directional pattern in horizontal plane and can be relatively easily manufactured. The characteristics of radiation pattern and gain of the sleeve antenna are the same with those of the dipole antenna.

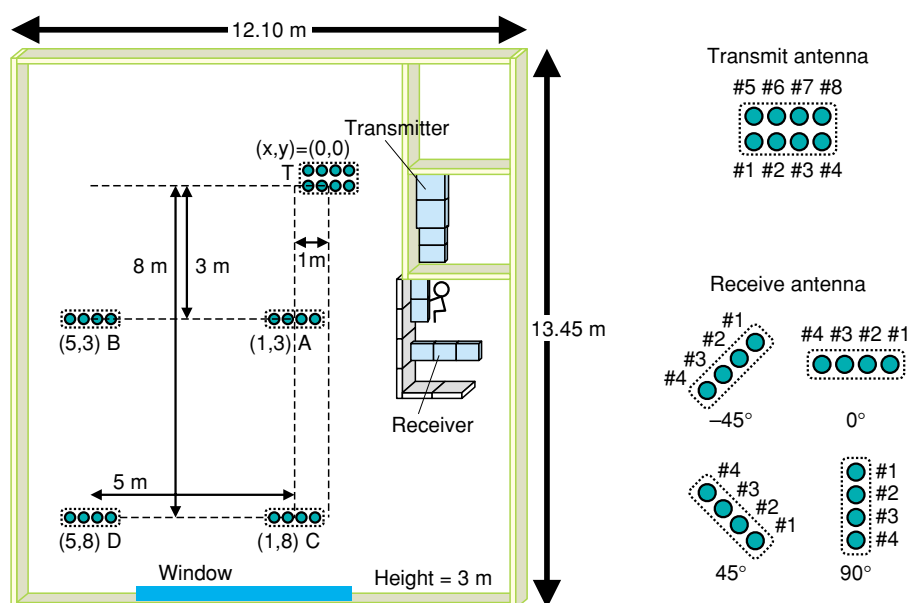


Fig. 6. Measurement environment.

Table 3. Number of antennas and SDM scheme.

Number of Tx and Rx	Transmit beamforming	Decoding algorithm
1, 1	None	None
1, 4	None	MRC
2, 2	None	ZF
2, 4		
3, 3		
3, 4		
4, 4		
4, 4	E-SDM	ZF
8, 4		

tion for one to four antennas are given when we evaluated the SDM scheme without transmit beamforming. We used the ZF algorithm, which is basically used as the decoding algorithm for the SDM scheme. When using the ZF algorithm, the number of streams equaled the number of receive antennas. We also evaluated  $4 \times 4$  and  $8 \times 4$  E-SDM, where the decoding algorithm was ZF with E-SDM.

In this measurement, we used the modulation signals given in Table 1 and the frame format in Fig. 3 with  $P = 50$ . The total number of bits was almost  $10^7$ , so the frequency utilization was obtained from the BER for almost  $10^7$  bits. The frequency utilization (2.7 bits/s/Hz, or 54 Mbit/s per 20 MHz) based on the 64QAM modulation scheme with coding rate  $R = 3/4$  in wireless LAN systems based on the IEEE802.11a standard was used as the standard. In this case, 4.5

bits per subcarrier per OFDM symbol could be transmitted. In this study, we regarded a signal with a BER of less than  $10^{-5}$  as being error-free, and we defined the point at which  $\text{BER} = 10^{-5}$  intersects the function fitting curve, which was obtained from the BER characteristics versus the transmission rate, as the frequency utilization.

### 3.2 Frequency utilization when applying ZF algorithm

In this sub-section, the performance of the ZF-SDM decoding scheme without transmit beamforming is evaluated. The BER characteristics versus frequency utilization for one to four transmit and receive antennas are shown in Fig. 7, which shows the results for receiving point A and a rotation angle of  $0^\circ$ . For  $2 \times 2$  MIMO transmission using the ZF algorithm, the frequency utilization was 1.8 times that for  $1 \times 1$  transmission. However, when the numbers of transmit and receive antennas were increased to greater than two, the frequency utilization did not exhibit a significant increase. This is because noise enhancement caused by the ZF algorithm completely suppressed the inter-stream interference when the number of streams was increased [3].

To resolve the above problems, researchers are investigating methods in which a larger number of receive antennas or other SDM decoding schemes are used [3], [13]. In this paper, we clarify the diversity effect at the receivers achieved by increasing the number of receive antennas to greater than the num-

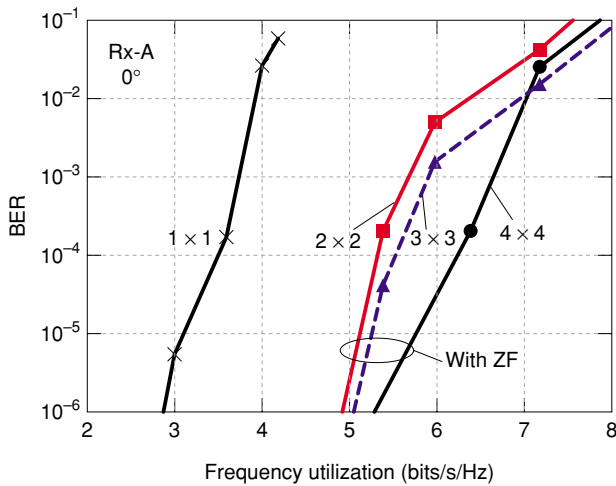


Fig. 7. BER versus frequency utilization (with ZF algorithm).

ber of streams. The frequency utilization versus the number of transmit and receive antennas is shown in Fig. 8. The frequency utilization could be improved by setting the number of receive antennas, but not the number of streams, to four. For example, 2 × 4 and 3 × 4 MIMO transmission with the ZF algorithm exhibited frequency utilization that was 2.3 and 2.5 times that for 1 × 1 transmission, respectively. Moreover, we could confirm that the frequency utilization of 3 × 4 SDM with the ZF algorithm was higher than that of 4 × 4 SDM with the ZF algorithm. Therefore, when the ZF algorithm without transmit beamforming is used for MIMO transmission, receive diversity is very effective in improving the frequency utilization.

### 3.3 Effectiveness of E-SDM transmission

The BER characteristics versus frequency utilization when applying the E-SDM scheme are shown in Fig. 9. Frequency utilization of 9.8 and 13.7 bit/s/Hz could be obtained using the 4 × 4 and 8 × 4 E-SDM schemes, respectively. These values correspond to improvements of 3.6 and 5.1 times the frequency utilization values for commercial wireless LAN systems based on IEEE802.11a. Moreover, the frequency utilization for the 8 × 4 E-SDM (13.7 bits/s/Hz) is the highest transmission rate reported to date in any official publication related to MIMO technology. These results were for a bandwidth of 20 MHz. When we set a 100-MHz bandwidth, which is the maximum that our testbed can handle, we obtained frequency utilizations of 11.2 and 15.2 bit/s/Hz using 4 × 4 and 8 × 4 E-SDM schemes, respectively, with a guard band of 4 MHz.

To clarify why 8 × 4 E-SDM could obtain such a

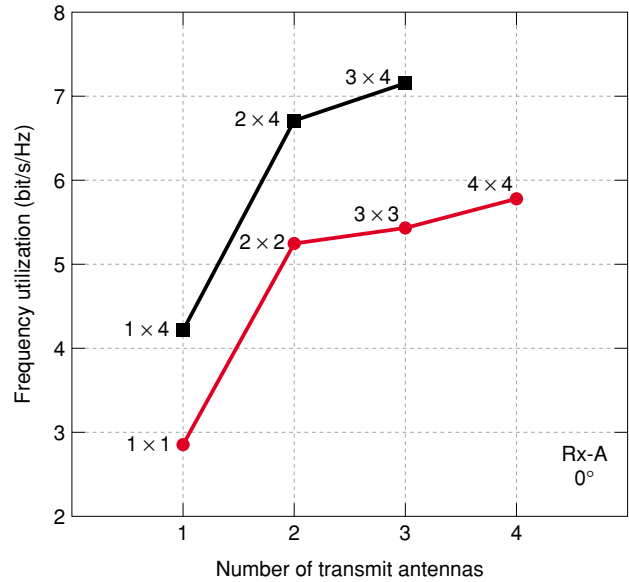


Fig. 8. Frequency utilization versus number of transmit antennas (Decoding algorithm is ZF).

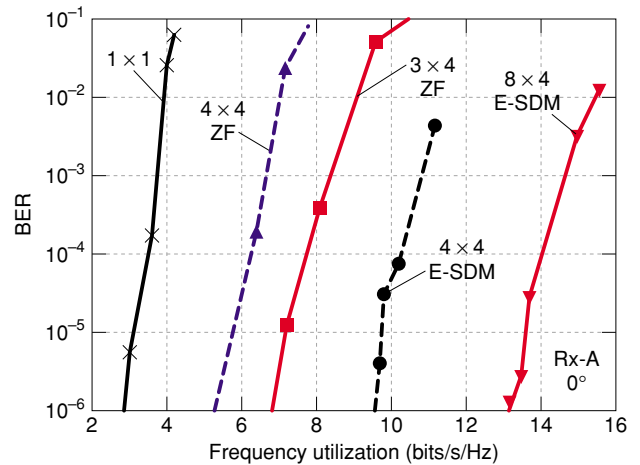


Fig. 9. BER versus frequency utilization with E-SDM.

high frequency utilization, we considered the eigenvalue distribution obtained by channel matrix  $H$ . The 1st to 4th eigenvalues versus the number of subcarriers in 4 × 4 and 8 × 4 MIMO channels, respectively, are shown in Fig. 10. The 4th eigenvalues changed greatly versus the number of subcarriers in 4 × 4 MIMO channels, and these values were about 1/1000 of the 1st eigenvalue. Thus, in this study, it was difficult to allocate the modulation schemes to the fourth stream in 4 × 4 E-SDM. On the other hand, the values of the 4th eigenvalue did not change much versus the number of subcarriers in 8 × 4 MIMO channels, and we could allocate 64QAM schemes to the fourth

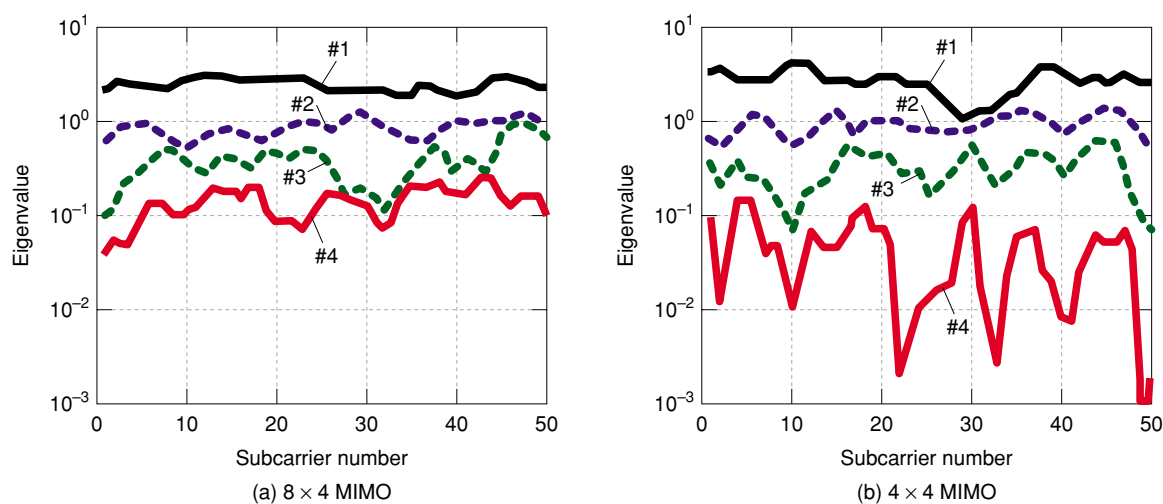


Fig. 10. Eigenvalue versus number of subcarriers.

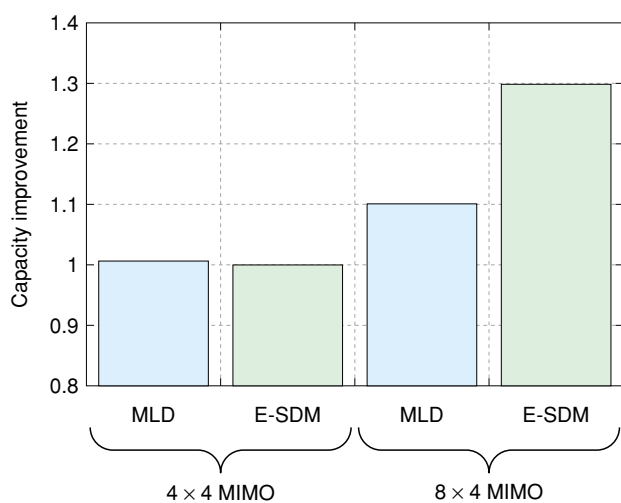


Fig. 11. Improvement in channel capacity using the eigenvalues obtained by the channel matrix.

stream in  $8 \times 4$  E-SDM transmission. Therefore,  $8 \times 4$  E-SDM could obtain the very high frequency utilization of 13.7 bits/s/Hz because we could utilize all four streams in  $8 \times 4$  MIMO channels.

The ideal channel capacity [5], which is obtained using all eigenvalues in  $8 \times 4$  and  $4 \times 4$  MIMO channels, respectively, is shown in **Fig. 11**. This result is based on the ideal reception decoding, and this channel capacity theoretically corresponds to that of MLD [3]. Furthermore, the channel capacity with  $4 \times 4$  E-SDM was normalized to one. As can be seen in **Fig. 11**, the channel capacity of E-SDM was almost the same as that of MLD in  $4 \times 4$  MIMO channels. On the other hand, E-SDM could improve the channel capacity by 1.3 times that for MLD in  $8 \times 4$  MIMO

Table 4. Frequency utilization comparison between E-SDM and SDM with ZF.

Measured point	Rotation angle ( $^{\circ}$ )	Frequency utilization (bits/s/Hz)		
		$8 \times 4$ E-SDM	$4 \times 4$ E-SDM	$3 \times 4$ ZF
A	-45	13.57	9.97	8.18
	0	13.74	9.86	7.13
	45	13.76	9.85	8.45
	90	13.88	9.66	7.74
B	-45	11.78	9.25	5.09
	0	12.66	9.44	5.05
	45	12.53	8.81	6.66
	90	12.31	8.87	5.71
C	-45	10.52	8.72	7.71
	0	12.14	8.76	7.28
	45	11.35	8.94	7.00
	90	10.94	8.71	6.28
D	-45	12.37	9.23	6.78
	0	12.14	8.62	6.96
	45	12.43	9.47	6.88
	90	12.21	9.72	7.24
Average		12.40	9.24	6.88

channels. Therefore, using E-SDM is very effective if the number of antennas at the access point is greater than the number of mobile terminals. Moreover, we could confirm that this improvement with  $8 \times 4$  E-SDM almost coincided with the result in **Fig. 9**.

The frequency utilizations at all receiving points and rotating angles when the  $8 \times 4$  E-SDM,  $4 \times 4$  E-SDM, and  $3 \times 4$  ZF schemes were used are shown in **Table 4**. The changes in frequency utilization were

mainly due to the differences at the receiving points or in the directions of the receive array antenna. This is because the spatial correlation characteristics between transmit and receive antennas changed when the directions or locations were changed, and the ZF algorithm had a significant effect on the spatial correlation characteristics. On the other hand, the deterioration due to the differences in directions and locations of the receive array antenna was relatively small compared with the ZF-SDM when E-SDM was used. From the average frequency utilization of all measured points, we could confirm that  $8 \times 4$  and  $4 \times 4$  E-SDM could obtain frequency utilization 1.8 and 1.35 times better than  $3 \times 4$  ZF.

Transmit beamforming such as E-SDM should not only improve the frequency utilization, but also expand the service area through its radiation pattern control. To confirm the improvement in the service area achieved by E-SDM, we evaluated the frequency utilization when the transmit power was changed. The frequency utilization versus transmit power for  $8 \times 4$  E-SDM and  $3 \times 4$  ZF is shown in Fig. 12. Transmit power of 0 dBm was necessary to obtain frequency utilization of 7.7 bits/s/Hz when  $3 \times 4$  ZF was used, but transmit power of  $-15$  dBm could achieve the same frequency utilization when  $8 \times 4$  E-SDM was used. This large reduction in transmit power (15 dB) shows that  $8 \times 4$  E-SDM will be very effective for expanding the service area. Moreover, since the peak-to-average-power ratio (PAPR) should be reduced in MIMO-OFDM systems, E-SDM should also be effective from this viewpoint.

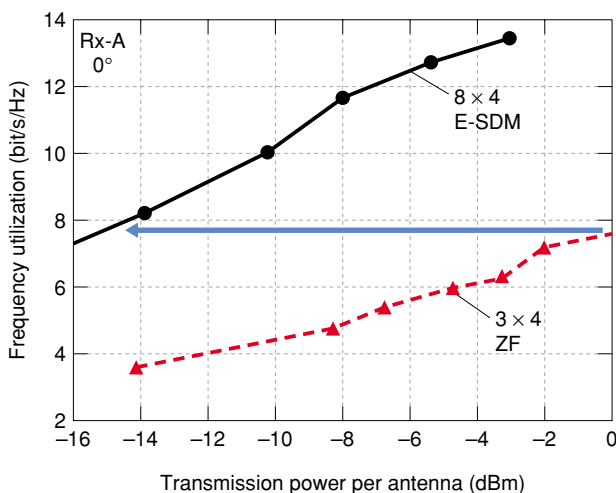


Fig. 12. Frequency utilization versus transmission power.

## 4. Conclusion

This paper described the features and basic characteristics of a broadband MIMO-OFDM testbed that can evaluate  $8 \times 4$  E-SDM transmission. This testbed can not only obtain the correlation and eigenvalue distribution, which are key parameters in MIMO channels, but also evaluate the transmission quality including the error correction used in MIMO-OFDM transmission. We evaluated the frequency utilization when using this MIMO-OFDM testbed in an actual indoor environment. Using  $8 \times 4$  E-SDM transmission, we obtained maximum frequency utilization of 13.7 bits/s/Hz, which is the highest value reported to date for MIMO-OFDM.

## References

- [1] G. L. Stuber, J. R. Barry, S. W. McLaughlin, Y. Li, M. A. Ingram, and T. G. Pratt, "Broadband MIMO-OFDM wireless communications," *Proceedings of IEEE*, Vol. 92, pp. 271-294, Feb. 2004.
- [2] S. Korosaki, Y. Asai, T. Sugiyama, and M. Umehira, "A SDM-COFDM scheme employing a simple feed-forward inter-channel interference canceller for MIMO based broadband wireless LANs," *IEICE Trans. Commun.*, Vol. E86-B, No. 1, pp. 283-290, Jan. 2003.
- [3] T. Ohgane, T. Nishimura, and Y. Ogawa, "Applications of space division multiplexing and those performance in a MIMO channel," *IEICE Trans. Commun.*, Vol. E88-B, No. 5, 1843-1851, May 2005.
- [4] A. Paulraj, R. Nabar, and D. Gore, "Introduction to Space-Time Wireless Communications," Cambridge University Press, 2003.
- [5] I. E. Telatar, "Capacity of multi-antenna Gaussian channels," *Euro. Trans. Telecommun.*, Vol. 1, No. 6, Nov./Dec. 1999.
- [6] J. B. Andersen, "Array gain and capacity for known random channels with multiple element arrays at both ends," *IEEE J. Sel. Areas Commun.*, Vol. 18, No. 11, pp. 2172-2178, Nov. 2000.
- [7] K. Miyashita, T. Nishimura, T. Ohgane, Y. Ogawa, Y. Takatori, and K. Cho, "High data-rate transmission with Eigenbeam Space Division Multiplexing (E-SDM) in a MIMO channel," *Proc. of IEEE VTC2002-Fall*, Vol. 3, pp. 1302-1306, 2002.
- [8] "MIMO implementation aspects," *IEEE Radio and Wireless Conference (RAWCON)*, Workshop WS2, Sep. 2004.
- [9] A. Zelst and T. C. W. Schenk, "Implementation of a MIMO OFDM based wireless LAN systems," *IEEE Trans. Signal Process.*, Vol. 52, No. 2, pp. 483-494, Feb. 2004.
- [10] K. Higuchi, H. Atarashi, J. Kawamoto, Y. Kawai, N. Maeda, and M. Sawahashi, "Overview of experimental system for achieving over 1-Gbps packet transmission using MIMO channel for broadband packet radio access," *2005 IEICE General Conference*, B-5-69, May 2005.
- [11] K. Sakaguchi, S. Ting, and K. Araki, "Initial measurement on MIMO eigenmode communication systems," *IEICE Trans. B*, Vol. J87-B, No. 9, pp. 1454-1466, 2004.
- [12] IEEE802.11.a, "High speed physical layer (PHY) in 5 GHz band," 1999.
- [13] K. Nishimori, R. Kudo, Y. Takatori, and K. Tsunekawa, "Performance evaluation of  $4 \times 4$  MIMO-OFDM testbed in an actual indoor environment (1) ~Overview of MIMO-OFDM testbed and basic characteristics~," *Technical Report of IEICE*, AP2004-296, Mar. 2005.
- [14] R. Kudo, K. Nishimori, Y. Takatori, and K. Tsunekawa, "Performance evaluation of  $4 \times 4$  MIMO-OFDM testbed in an actual indoor environment (2) ~Improvement on transmission quality by using eigen-mode transmission~," *Technical Report of IEICE*, AP2004-297, Mar. 2005.


**Kentaro Nishimori**

Research Engineer, Wireless Systems Innovation Laboratory, NTT Network Innovation Laboratories.

He received the B.E., M.E., and Dr.Eng. degrees in electrical and computer engineering from Nagoya Institute of Technology, Nagoya, Aichi in 1994, 1996, and 2002, respectively. He joined NTT Wireless Systems Laboratories in 1996. He received the Young Engineers Award from the Institute of Electronics, Information and Communication Engineers (IEICE) of Japan in 2001 and Young Engineer Award from IEEE AP-S Japan Chapter in 2001. His current research interest is smart antennas for mobile communications and MIMO systems. He is a member of IEEE and IEICE.


**Riichi Kudo**

Engineer, Wireless Systems Innovation Laboratory, NTT Network Innovation Laboratories.

He received the B.E. and M.E. degrees in geophysics from Tohoku University, Sendai, Miyagi in 2001 and 2003, respectively. He joined NTT Network Innovation Laboratories in 2003. His current research interest is MIMO communication systems. He is a member of IEICE.


**Yasushi Takatori**

Research Engineer, Wireless Systems Innovation Laboratory, NTT Network Innovation Laboratories.

He received the B.E. degree in electrical and communication engineering and the M.E. degree in system information engineering from Tohoku University, Sendai, Miyagi in 1993 and 1995, respectively. He joined NTT Wireless Systems Laboratories in 1995. He was a visiting researcher at the Center for TeleInfrastruktur (CTIF), Aalborg University, Aalborg, Denmark from 2004 to 2005. He received the Young Engineers Award from IEICE in 2000, the Excellent Paper Award of WPMC (International Symposium on Wireless Personal Multimedia Communications) in 2004, and the YRP (Yokosuka Research Park) Award in 2005. His current research interests are smart antennas, MIMO systems, and spatial signal processing techniques. He is an associate editor of the Springer Journal of Wireless Personal Communications. He is a member of IEEE and IEICE.


**Koichi Tsunekawa**

Senior Manager, Wireless Systems Innovation Laboratory, NTT Network Innovation Laboratories.

He received the B.S., M.S., and Ph.D. degrees in engineering science from the University of Tsukuba, Tsukuba, Ibaraki in 1981, 1983, and 1992, respectively. He joined the Electrical Communications Laboratories of Nippon Telegraph and Telephone Public Corporation (now NTT), Tokyo in 1983. Since 1984, he has been engaged in R&D of portable telephone antennas in land mobile communication systems. From 1993 to 2003, he was with NTT DoCoMo, Inc. where he worked on radio propagation research, intelligent antenna systems for wireless communications, and the developing IMT-2000 antenna systems. His research interests are antenna systems for MIMO transmission, millimeter-wave broadband access, and ubiquitous wireless systems. He is a member of IEICE and IEEE.